JCTC Journal of Chemical Theory and Computation

Blending Determinism with Evolutionary Computing: Applications to the Calculation of the Molecular Electronic Structure of Polythiophene

Kanchan Sarkar, Rahul Sharma, and S. P. Bhattacharyya*

Department of Physical Chemistry, Indian Association for the Cultivation of Science, Jadavpur, Kolkata-700032, India

Received October 13, 2009

Abstract: A density matrix based soft-computing solution to the quantum mechanical problem of computing the molecular electronic structure of fairly long polythiophene (PT) chains is proposed. The soft-computing solution is based on a "random mutation hill climbing" scheme which is modified by blending it with a deterministic method based on a trial single-particle density matrix [$\mathbf{P}^{(0)}(R)$] for the guessed structural parameters (R), which is allowed to evolve under a unitary transformation generated by the Hamiltonian $\mathbf{H}(R)$. The Hamiltonian itself changes as the geometrical parameters (R) defining the polythiophene chain undergo mutation. The scale (λ) of the transformation is optimized by making the energy [$E(\lambda)$] stationary with respect to λ. The robustness and the performance levels of variants of the *algorithm* are analyzed and compared with those of other derivative free methods. The method is further tested successfully with optimization of the geometry of bipolaron-doped long PT chains.

1. Introduction

Exact solutions of the Schrodinger equation for many-electron systems are impossible to obtain analytically. The solutions are therefore obtained by various approximation methods, which are still rather complicated for applications to large systems. With rapid and spectacular advances in digital computing, computational methods of electronic structure calculations have attracted serious attention in recent years.[1−3] These methods have become practically essential for understanding large systems at the microscopic level. Finding efficient algorithms for handling large quantum systems even at an approximate level has become a challenging issue. Traditional electronic structure algorithms calculate eigenstates associated with discrete energy levels, and this leads to a diagonalization problem of the Hamiltonian matrix. The computational effort in traditional diagonalization methods scales as N^3, where N is the dimension of the basis space. Usually one is interested in finding the lowest energy structure so that one has to simultaneously search the potential energy surface $E(R)$ for locating the global minimum while diagonalizing the Hamiltonian matrix $\mathbf{H}(R)$ at different geometries (R).

In the present paper we have proposed a novel nondeterministic *algorithm* for locating the minimum energy structures of neutral or doped PT chains of 100, 150, and 200 thiophene rings. To be specific, we have proposed a variant of the "directed random mutation hill climbing (DRMHC) method",[14,15] which works with a randomly generated string of all the geometrical parameters (nuclear position variables, R) required to compute the energy and therefore the fitness of a neutral or doped PT molecule within the framework of a modified SSH effective π-electron Hamiltonian model.[12,13] The geometry string $\{R_i\}$ is allowed to undergo directed random mutations. The string of mutated geometry variables $\{R_i'\}$ is used to define the Hamiltonian $\mathbf{H}(\{R_i'\})$, which acts as the generator of a unitary transformation, $\mathbf{U}(\lambda,\{R_i'\})$. $\mathbf{U}(\lambda,\{R_i'\})$ transforms a trial one-electron density matrix ($\mathbf{P}^{(0)}$) into a "mutated" one-electron density matrix ($\mathbf{P}^{(0)\prime}$), which is used to compute the "energy" of the mutated structure and hence the fitness of the structure coded by the mutated geometry string. The parameter λ fixes the scale of the transformation which is optimized at each random mutation hill climbing step by making the energy stationary with

* Corresponding author fax: (91)332473 2805; e-mail: pcspb@iacs.res.in.

10.1021/ct900540d
Published on Web 02/01/2010

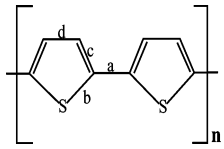

Figure 1. Fragment of the thiophene chain: (a) C−C bridging bond, (b) C−S single bond, (c) C−C double bond, (d) C−C single bond.

Table 1. Parameters in the SSH Hamiltonian (for Polythiophene) Used in These Calculations

param	value	description
A	123.6 eV	Hamiltonian parameter
B	0.3776 au	Hamiltonian parameter
D	7.814 au^{-1}	Hamiltonian parameter
$R^0_{(C-C)}$	1.557 au	C−C single bond length
$R^0_{(C-S)}$	1.782 au	C−S bond length
$R^0_{(C-C)B}$	1.557 au	C−C bridging bond length

respect to λ. We note here that there have been a number of earlier attempts to calculate the one- and two particle-density matrices using similar unitary transformations[8−10] on a trial density. We have, to the best of our knowledge, tried for the first time to blend it with an otherwise stochastic approach for computing the one-electron density matrix. We have compared the λ-optimized DRMHC algorithm with several alternative soft-computing methods of solving the problem. The algorithm is elaborately tested on long polythiophene chains, undoped as well as doped, and the results are briefly analyzed.

The outline of the paper is as follows. In section 2 we present the *algorithm* in detail, while the results of the applications are described in section 3. Section 4 presents the concluding remarks.

2. Method

Polythiophene (PT) oligomers have attracted the widespread attention of experimentalists and theoreticians because these molecules and their derivatives are capable of displaying metallic conduction under electron or hole doping.[4−7,11−13] Neutral PTs are chemically stable, can be synthesized easily, and can be doped with dopants such as ClO_4 and AsF_5. The stability remains intact even after doping.

The UV photoelectron spectrum[5] of neutral PT shows the existence of two π-bands in the system, and the Fermi level is ∼1.2 eV above the valence band (VB). There are two nondegenerate classical resonating forms of PT in which the $2p_z$ orbitals of the carbon atoms and the $3p_z$ orbitals of the sulfur atoms interact to form a π-band, half of which is occupied by the electrons. Had the two forms been isoenergic, a solitonic mode of conduction would have been viable as the solitons have a tendency to separate because the structure between the defects is isoenergic with the structure outside. However, in PT, the degeneracy is weakly lifted, and as a consequence the solitonic mode of conduction is ruled out. It turns out that polarons and bipolarons are the most important excitations and charge-storage configurations in doped PT.[6]

While PT is a semiconductor with a band gap of about 2 eV, hole doping reduces the gap, and at high doping levels PT begins to show metallic properties. It is important therefore to understand how the electronic structure of neutral PT evolves under doping. It is expedient in this context to have algorithms that can locate the global minimum energy structures on the potential energy surface of PT oligomers, undoped or doped. There are several deterministic methodologies, mostly based on a gradient search, which have been explored for locating the minimum energy structures of PTs.[6,7] Rarely, however, nondeterministic techniques have been explored in this context.[11] Our primary concern here is to introduce such a hybrid technique of geometry optimization and calculation of electronic structure and test its workability with undoped and doped PTs as examples.

PT is treated as a conjugated polyene and described by a tight binding model of the π-electronic system that includes only the nearest neighbor hopping interactions. The lattice dynamics is treated classically. This leads to a modified SSH effective π-electronic Hamiltonian $\mathbf{H}$ where[12,13]

$$\mathbf{H} = \mathbf{H}_e^{\pi} + \mathbf{H}_l^{\sigma} \tag{1}$$

The π-electronic Hamiltonian ($\mathbf{H}_e^{\pi}$) is expressed as

$$\mathbf{H}_e^{\pi} = \sum_n \alpha_n a_n^{\dagger} a_n + \frac{1}{2}\sum_{n,m} V_{nm} a_n^{\dagger} a_m + hc \tag{2}$$

and the lattice Hamiltonian (the σ-electronic framework Hamiltonian) is defined as

$$\mathbf{H}_l^{\sigma} = \sum_n \frac{p_n^{\,2}}{2M_n} + \frac{1}{2}\sum_{n,m} f(R_{nm}) \tag{3}$$

α_n is the self-energy of the carbon $2p_z$ electron ($3p_z$ electron of sulfur) at the nth site, and V_{nm} represents the hopping interaction between the nth and mth sites. V_{nm} is parametrized in the form[7,11]

$$\begin{aligned} V_{nm} &= -Ae^{-R_{nm}/B} && (|n-m| = 1) \\ &= 0 && (\text{otherwise}) \end{aligned} \tag{4}$$

with two parameters, A and B. R_{nm} is the distance separating the nth and mth adjacent sites. We use frozen core approximation so that the kinetic energy of the lattice is zero, i.e.

$$\mathbf{H}_l^{\sigma} = \frac{1}{2}\sum_{n,m} f(R_{nm}) \tag{5}$$

where

$$f(R_{nm}) = -AD_{nm}(R_{nm} - R_{nm}^0 + B)e^{-R_{nm}/B}$$

A, B, and D_{nm} are parameters of the model and R_{nm}^0 is the standard length of the $n-m$ bond.[7,11]

We start by guessing randomly the M number of bond lengths required to describe the N_r-ring chain, forming and diagonalizing the N-dimensional ($N = 5N_r$) π-electron Hamiltonian $\mathbf{H}_e^{\pi}$ in the N-dimensional basis of the carbon $2p_z$ and sulfur $3p_z$ atomic orbitals of all the carbon and sulfur atoms of the chain. The diagonalization generates a set of N π molecular orbitals $\{\phi_i\}$, N_{oc} of which are occupied by the

π-electrons in pairs ($N_{oc} = 3N_r$). In general, we can write the π MOs $\{\phi_i\}$ as linear combinations of the atomic basis orbitals (χ_p), where

$$\phi_i = \sum_{p=1}^{N} c_{p_i}\chi_p$$
$$\mathbf{H}_e^{\pi}\phi_i = \varepsilon_i^{\pi}\phi_i,\ i = 1, 2, ..., N \tag{6}$$

ε_i^{π} represent the binding energies of the π molecular electrons. The linear expansion coefficients $\{c_{p_i}\}$ define the elements of the charge density bond order matrix $\mathbf{P}$ through the relation

$$\mathbf{P}_{pq} = \sum_{i=1}^{N_{oc}} c_{p_i} c_{q_i}^{*} \tag{7}$$

so that the starting density matrix is defined as

$$\mathbf{P}^{(0)} = \sum_{i=1}^{N_{oc}} c_i^0 c_i^{0\dagger} \tag{8}$$

$\mathbf{P}^{(0)}$ satisfies the following constraints:

$$\mathbf{P}^{(0)\dagger} = \mathbf{P}^{(0)},$$
$$2\ \mathrm{Tr}\,\mathbf{P}^{(0)} = N_e, \quad (N_e = 6N_r)$$
$$(\mathbf{P}^{(0)})^2 = \mathbf{P}^{(0)} \tag{9}$$

where N_e is the number of electrons. The ground-state π-electronic energy E_G^{π} is given by

$$E_G^{\pi} = \sum_{k=1}^{N_{oc}} n_k \varepsilon_k^{\pi} = 2\sum_{n=1} \alpha_n q_n^0 + 2\sum_{n<m}\sum_{m} V_{nm}\mathbf{P}_{nm}^0 \tag{10}$$

q_n^0 is the electronic charge density at the nth site (diagonal elements of $\mathbf{P}^{(0)}$ formed in the atomic orbital basis). The total energy of the π-electron system including the elastic deformation energy of the σ-electronic framework is given by

$$E_T(R) = E_G^{\pi} + E_{\sigma} = E_G^{\pi} + \frac{1}{2}\sum_{n,m} f(R_{nm}) \tag{11}$$

Our purpose is to find the set of $\{R_{nm}\}$ values that globally minimize the ground-state energy $E_T(R)$ and calculate the corresponding charge density bond order matrix ($\mathbf{P}$) that encodes the equilibrium charge distribution in the ground state. We suggest the following strategy for solving the problem.

Let the geometrical parameters $\{R_{nm}\}$ defining the PT chain form a string $s(R_1, R_2, R_3, ..., R_k, ..., R_m, ..., R_M)$, where M is the total number of bonds in the system. The π-electronic Hamiltonian $\mathbf{H}_e^{\pi}(R)$ for the guessed geometry coded by the string $s(R)$ is diagonalized in the basis of the $2p_z$ orbitals of the carbon atoms and $3p_z$ orbitals of the sulfur atoms, and a trial density $\mathbf{P}^{(0)}(R)$ is generated. We choose one of the parameters, say the kth parameter, randomly with a

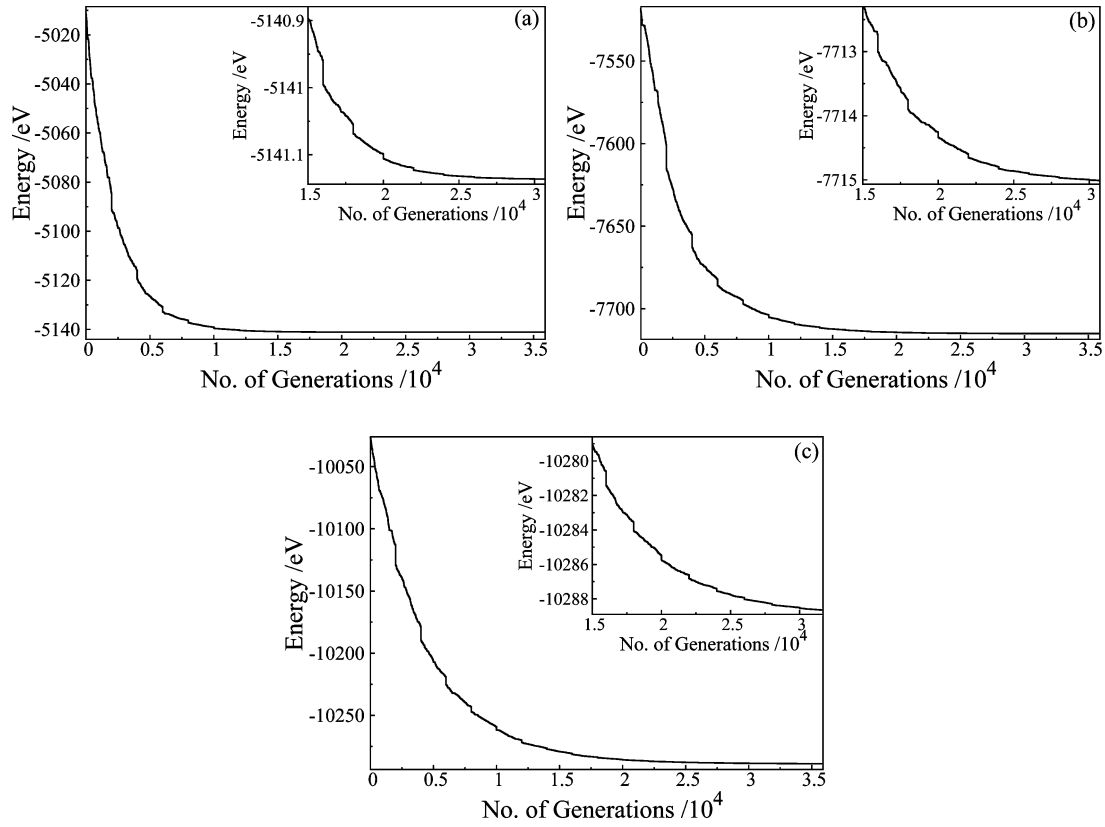

Figure 2. Energy evolution profiles of PT chains in the λ-optimized density matrix based DRMHC method (the inset figures display the fitness evolution between 15000 and 30000 generations in all the cases of 100-, 150-, and 200-ring PT chains): (a) for the 100-ring chain, (b) for the 150-ring chain, (c) for the 200-ring chain.

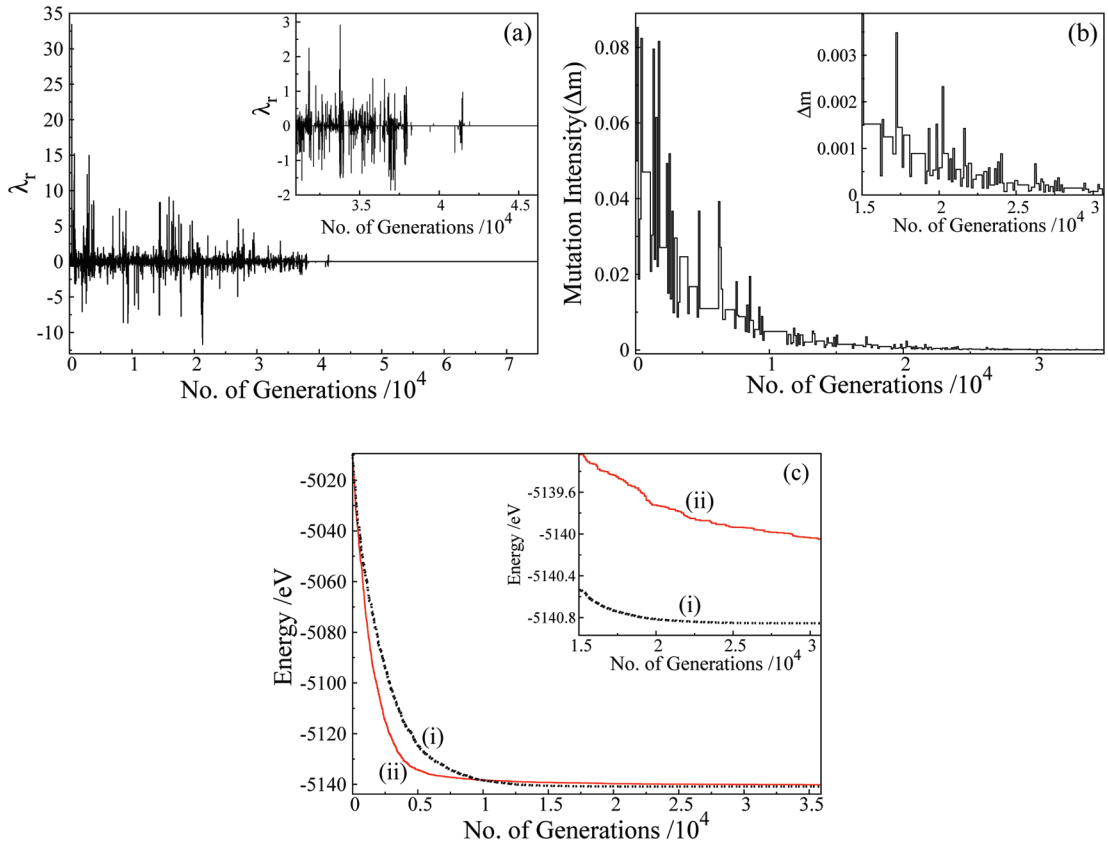

Figure 3. For a PT chain containing 100 rings: (a) evolution of λ_r in the λ-optimized density matrix based DRMHC scheme (the inset figure displays the evolution of λ_r between 30000 and 45000 generations), (b) evolution of Δ_m in the DRMHC scheme, (c) (i) energy evolution profiles in the DRMHC method at fixed $\lambda = 0.1$ (in the inset the evolution between 15000 and 30000 generations is shown to emphasize the different rates of the evolution in the convergence region), (ii) energy evolution profiles in the RMHC method at fixed $\Delta_m = 0.05$ (the inset shows the evolution profile between 15000 and 30000 generations).

probability p_m for mutation. The mutation induces a small change in the chosen parameter (R_k) in the following manner:[16]

$$R'_k = R_k + (-1)^l \Delta_m r$$

where l is a random integer, r is a random number in the range (0, 1), and Δ_m is a directed mutation intensity[17] (see later). The mutated string $s(R_1, R_2, R_3, ..., R'_k, ..., R_m, ..., R_M)$ is used to generate the π-electron Hamiltonian $\mathbf{H}_e^\pi(R')$, which in turn generates the unitary transformation matrix

$$\mathbf{U}_\lambda = e^{-i\lambda \mathbf{H}_e^\pi(R')} \tag{12}$$

where λ defines the scale of the transformation. The mutated density matrix $\mathbf{P}^{(1)}(R')$ is generated by transforming $\mathbf{P}^{(0)}(R)$ with $\mathbf{U}_\lambda$ in the following manner:[18]

$$\begin{aligned}\mathbf{P}^{(1)}(R') &= \mathbf{U}_\lambda \mathbf{P}^{(0)}(R) \mathbf{U}_\lambda^\dagger \\ &= e^{-i\lambda \mathbf{H}_e^\pi(R')}\, \mathbf{P}^{(0)}(R)\, e^{i\lambda \mathbf{H}_e^\pi(R')}\end{aligned} \tag{13}$$

Expanding the exponentials in powers of λ, we have (up to second order in λ)

$$\mathbf{P}^{(1)}(R') \approx \mathbf{P}^{(0)}(R) - i\lambda[\mathbf{P}^{(0)}(R), \mathbf{H}_e^\pi(R')] - \frac{\lambda^2}{2!}[[\mathbf{P}^{(0)}(R), \mathbf{H}_e^\pi(R')], \mathbf{H}_e^\pi(R')] \tag{14}$$

In eq 14, [**A**, **B**] represents the commutator of matrices **A** and **B**. The problem now is to fix the scale parameter λ. We do that by estimating the electronic energy $\varepsilon_{el}^\pi(\lambda)$ and making it stationary with respect to variations in λ. Thus, using $\mathbf{P}^{(1)}$ to estimate $\varepsilon_{el}^\pi(\lambda)$, we have, up to second order in λ

$$\begin{aligned}\varepsilon_{el}^\pi(\lambda) &\approx 2\,\mathrm{Tr}\{\mathbf{P}^{(1)}\,\mathbf{H}_e^\pi(R')\} \\ &= 2[\mathrm{Tr}\{\mathbf{P}^{(0)}\,\mathbf{H}_e^\pi(R')\}] - i\lambda\,\mathrm{Tr}\{[\mathbf{P}^{(0)}, \mathbf{H}_e^\pi(R')]\mathbf{H}_e^\pi(R')\} - \frac{\lambda^2}{2!}\mathrm{Tr}\{[[\mathbf{P}^{(0)}, \mathbf{H}_e^\pi(R')], \mathbf{H}_e^\pi(R')]\mathbf{H}_e^\pi(R')\}\end{aligned}$$

Setting

$$\frac{\partial \varepsilon_e^\pi(\lambda)}{\partial \lambda} = 0 \tag{15}$$

then leads to

$$\lambda_{opt} = -i\frac{\mathrm{Tr}\{[\mathbf{P}^{(0)}, \mathbf{H}_e^\pi(R')]\mathbf{H}_e^\pi(R')\}}{\mathrm{Tr}\{[[\mathbf{P}^{(0)}, \mathbf{H}_e^\pi(R')], \mathbf{H}_e^\pi(R')]\mathbf{H}_e^\pi(R')\}} \tag{16}$$

$$= -i\lambda_r \tag{17}$$

where

$$\lambda_r = \frac{\mathrm{Tr}\{[\mathbf{P}^{(0)}, \mathbf{H}_e^\pi(R')]\mathbf{H}_e^\pi(R')\}}{\mathrm{Tr}\{[[\mathbf{P}^{(0)}, \mathbf{H}_e^\pi(R')], \mathbf{H}_e^\pi(R')]\mathbf{H}_e^\pi(R')\}} \tag{18}$$

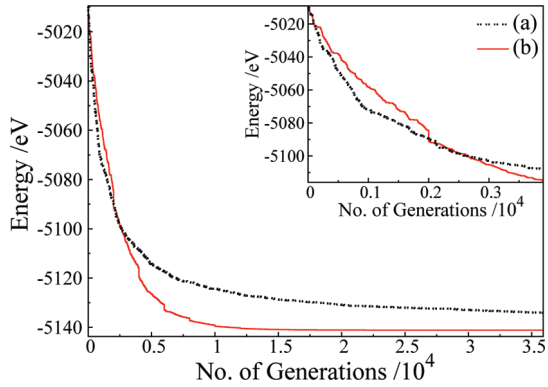

Figure 4. Comparison between the repeated diagonalization based RMHC procedure in the case of a 100-ring PT chain (a) and the λ-optimized density matrix based DRMHC method (b) (the inset shows that up to 3000 generations the two schemes perform in more or less the same way).

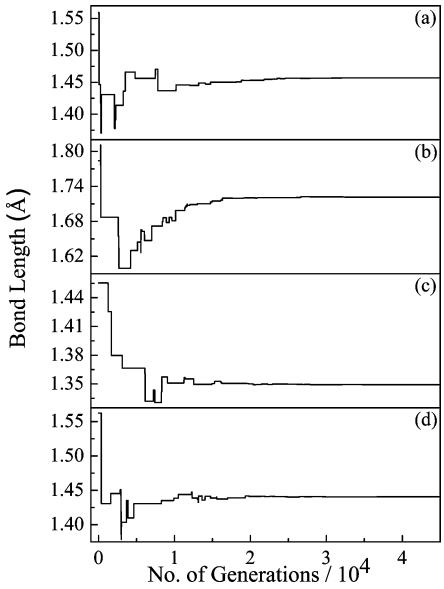

Figure 5. Bond length evolution profiles of 100-ring PT chains in the λ-optimized DRMHC method: (a) C−C bridging bond, (b) C−S single bond, (c) C−C double bond, (d) C−C single bond.

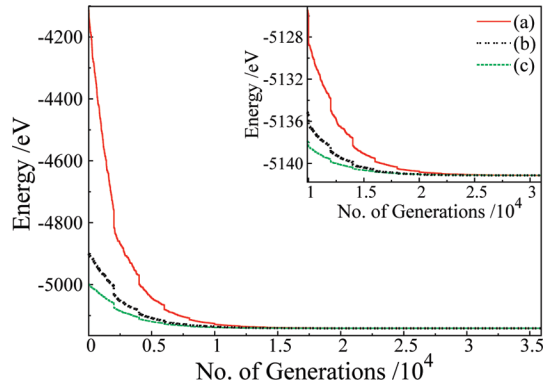

Figure 6. Convergence profiles with different starting points suggest that the λ-optimized density matrix based DRMHC process is robust (the inset shows profiles in the region between 9900 and 27000 generations). The molecule studied is a 100-ring PT chain.

If the total energy of the mutated structure $E'_T(R') = \varepsilon'^{\pi}_e + \varepsilon'_\sigma$ computed with λ_{opt} is lower (or the absolute value of $E'_T(R')$, which we call fitness, is higher) than the premutation energy $E_T(R)$, the mutated geometry string $s\{R'_i\}$ replaces the old string $s\{R_i\}$. If the condition is not satisfied, a new mutation site is chosen on the old string; thus, the algorithm avoids evolving nonviable candidates. In either case, one generation is counted to have elapsed. We may note here that $\mathbf{P}^{(1)}(R')$ of eq 13 is strictly idempotent while $\mathbf{P}^{(1)}(R')$ of eq 14 may not be so because of truncation. Also 2 Tr $\mathbf{P}^{(1)}(R')$ may deviate from the total number of electrons. Therefore, these quantities are followed throughout the evolution and corrective measures taken if required (through standard trace purification or idempotency-correcting routines).

The directed mutation scheme used in the present case[17] uses a mutation intensity that is dynamically adjusted on the basis of the degree of acceptability of mutation over a number of past generations. Thus, if the number of accepted mutations in the last 100 generations is less than 10, Δ_m is lowered to $\Delta'_m = \Delta_m/(1 + r)$ (r is a random number between 0 and 1). It is enhanced to $\Delta'_m = \Delta_m/(1 - r)$ if the number of accepted mutations is greater than 20 in the last 100 generations. Δ_m is kept unchanged otherwise.

The process is continued until the total energy stops evolving further. The equilibrium ground-state structure is represented by the geometry variables that the string $s(R_1, R_2, R_3, ..., R_M)$ corresponding to the converged energy or fitness encodes. The same algorithm can be extended to determine the electronic structure of doped PTs or other similar molecules.

3. Results and Discussion

We have considered specific cases of polythiophene oligomers containing 100, 150, or even 200 rings in a chain which require 599, 899, and 1199 bond lengths or geometry variables, respectively, to define the SSH Hamiltonian.[12,13] The geometry strings $s(R)$ encoding the structures of PT oligomers are arrays containing 599, 899, and 1199 floating point variables, respectively. We have experimented with several variants of the *algorithm* proposed in section 2, a few of which are reported here. The parameters of the SSH Hamiltonian used in these calculations are reported in Table 1.

3.1. Geometry Optimization in Neutral Polythiophene Oligomers. Let us consider a 100-ring undoped PT chain. In our λ-optimized DRMHC algorithm, we start with a geometry string in which the geometry variables are allowed to be distributed randomly over a predefined range. The mutation probability p_m is set to have a value $p_m = 5/M$, where M is the total number of bonds in the system, and held fixed throughout the evolution. The initial mutation intensity or rate (Δ_m) is assumed to be 0.05. Empirically Schaffer et al.[19] found that the optimum mutation rate in a genetic algorithm (GA) can be represented by the formula

$$\ln(N) + 0.93 \ln(\Delta_m) + 0.45 \ln(n) = 0.56 \qquad (19)$$

where N = size of the population, Δ_m = mutation rate, and n = length of the chromosome. Hesser et al.[20] provided a

heuristic argument in support of the empirical formula. The initial value of Δ_m chosen by us happens to be around half of the empirically estimated value of Δ_m (optimum) predicted by eq 19 if we assume that n represents the number of parameters present in a geometry string used here. The π-electronic Hamiltonian ($\mathbf{H}_e^{\pi}$) is diagonalized once after every 2000 generations. The parameter λ of the unitary transformation is optimized as outlined in section 2 (eq 16).

Figure 1 shows various bonds in the PT chain. Parts a−c of Figure 2 show how energy evolves during the density matrix based λ-optimized DRMHC search for the thiophene chain containing 100, 150, and 200 rings, respectively. In about 15000 generations, the search locates the gross features of the equilibrium structure in each case. The typical evolution pattern of λ_r (eq 18) for the representative case of λ optimization in the case of a 100-ring neutral PT chain is profiled in Figure 3a.

There are wide fluctuations in the scale parameter λ_r from one generation to another. As the search converges to the equilibrium structure the fluctuations get strongly damped and $\lambda_r \rightarrow 0$. Far away from the global minimum large λ_r is predicted to have a large magnitude. In a sense, this amounts to emphasizing the breadth search aspect of the algorithm. As the search approaches the global minimum, $\lambda_r \rightarrow 0$, thereby emphasizing the depth search aspect. The corresponding evolution profile of directed mutation intensities is depicted in Figure 3b. To understand the role played by λ-optimization, we have reported a second set of calculations on 100-ring PT chains in which λ_r is kept fixed at $\lambda_{av} = 0.1$ while all other parameters of the algorithm remain unaltered. The search failed to converge to the desired level, indicating the importance of λ-optimization in conjuction with a DRMHC search (Figure 3c). Similarly, another set of calculations were carried out with fixed mutation intensity ($\Delta_m = 0.05$) to understand the role played by directed mutation (Figure 3d). Again the search failed to hit the global minimum energy structure. We have checked that the trace of the density matrix and its idempotent character remain conserved to the desired accuracy throughout the evolution. Therefore, additional computational labor for purifying the "trace" or restoring the idempotency of $\mathbf{P}^{(1)}(R')$ of eq 14 was avoided. The transformation shown in eq 13 thus remains unitary for all practical purposes after the truncation shown in eq 14.

The performance of the λ-optimized DRMHC technique has also been compared with that of the conventional repeated diagonalization based procedure. Here $\mathbf{H}_e^{\pi}$ was diagonalized following every successful mutation step, and a new $\mathbf{P}^{(0)}$ was calculated directly from the eigenvectors of $\mathbf{H}_e^{\pi}$, bypassing the construction of and transformation with the unitary matrix $\mathbf{U}(\lambda,\{R_i\})$. It can be seen that the repeated diagonalization based RMHC procedure (Figure 4a) and density matrix based λ-optimized DRMHC (Figure 4b) algorithm perform more or less identically in the initial phase of evolution (first 3000 generations or so). Beyond that point density matrix based λ-optimized DRMHC performs better (Figure 4). We may mention that the maximum number of diagonalizations required in density matrix based λ-optimized DRMHC is between 10 and 20, while the repeated diagonalization RMHC procedure requires between 40000 and 45000 diagonalizations. Even then, the repeated diagonalization based RMHC procedure fails to hit the global minimum energy structure. The results are summarized in Table 2.

Parts a−d of Figure 5 display how the different geometry variables evolve during a search in the density matrix based λ-optimized DRMHC scheme for a PT chain containing 100

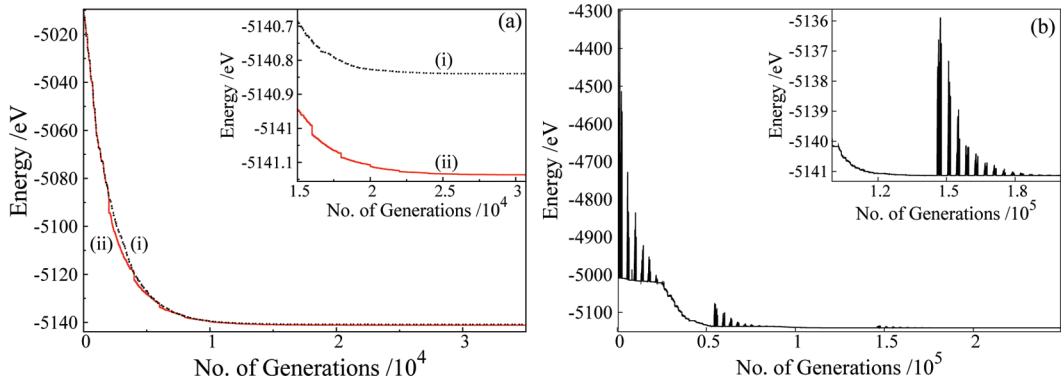

Figure 7. Energy evolution profiles of 100-ring PT chains with (a) (i) the GA (the inset shows the profile in the region between 15000 and 30000 generations) and (ii) the restricted crossover GA (crossover operation is restricted up to 2500 generations) (the inset shows the profile in the region between 15000 and 30000 generations) and (b) simulated annealing, with the inset representing the profile in the region between 99900 and 199900 generations.

Table 2. Comparison of the λ-Optimized Density Matrix Based DRMHC Method with the Repeated Diagonalization Based RMHC Procedure and Other Derivatives of the Density Matrix Based RMHC Scheme

scheme used	energy (eV)	no. of generations required	comment
λ-optimized DRMHC	−5141.137	37565	smooth and fast
DRMHC with fixed λ ($\lambda = 0.1$)	−5140.855	65201	gets stuck close to the global minimum
RMHC with fixed mutation intensity ($\Delta_m = 0.05$)	−5140.320	49375	fails to find the global minimum structure
repeated diagonalization	−5135.216	44752	fails to converge to the global minimum

Table 3. Comparison of the Performance of the λ-Optimized Density Matrix Based DRMHC Method and Other Soft-Computing Methods

scheme used	energy (eV)	no. of energy evaluations or iteration steps required	comment
simulated annealing method	−5141.137	240000	
genetic algorithm	−5141.137	67638	
genetic algorithm with restricted crossover	−5141.137	35539	costly but converges

rings. There are wide fluctuations in the bond lengths in the initial phase, which gradually get damped as the search converges.

To test the robustness and stability of the algorithm, the calculations have been performed with widely different starting geometries on the potential energy surface. The performance was slightly worse or better in different runs with different inputs (Figure 6), but convergence was achieved in each case. The average performance level closely matches with what has been reported in this paper.

3.2. Comparison with Other Soft-Computing Methods. The energy evolution of the density matrix based λ-optimized DRMHC method has been compared with what one actually observes with a density matrix based GA with a population size of 4 and the density matrix based simulated annealing method (SAM).[18] The convergence profiles of fitness/energy obtained with the GA and SAM are displayed in parts a and c, respectively, of Figure 7 for the geometry optimization of a 100-ring neutral PT chain. We note that the λ-optimized DRMHC method outperforms the two other soft-computing methods in terms of the number of steps needed to reach the minimum energy structure. In the case of the GA, the crossover operation is expected to help in the achievement of faster convergence, which is indeed noticed in the initial stages; however, the convergence to the global minimum is delayed. We have also compared the performance of a GA with restricted crossover (crossover allowed initially up to a limited number of generations) with that of the density matrix based λ-optimized DRMHC procedure (Figure 7b). It is observed that the restricted crossover GA provides approximately the same performance as obtained with the λ-optimized DRMHC scheme. DRMHC is nevertheless computationally economic as it needs only one string evaluation per generation, whereas in the GA fitness evaluation of a population of strings (four here) is to be carried out in every generation. The performance statistics are reported in Table 3. The scale optimized density matrix based DRMHC method has also been used to compute the global minimum energy structures of neutral PT chains of 150 and 200 rings. The predicted equilibrium geometrical parameters are reported in Table 4. The predicted lengths are practically identical. We did not enforce any symmetry constraint on the chain. Every geometrical parameter was allowed to evolve freely. The symmetry appeared naturally as the search converged to the global minimum.

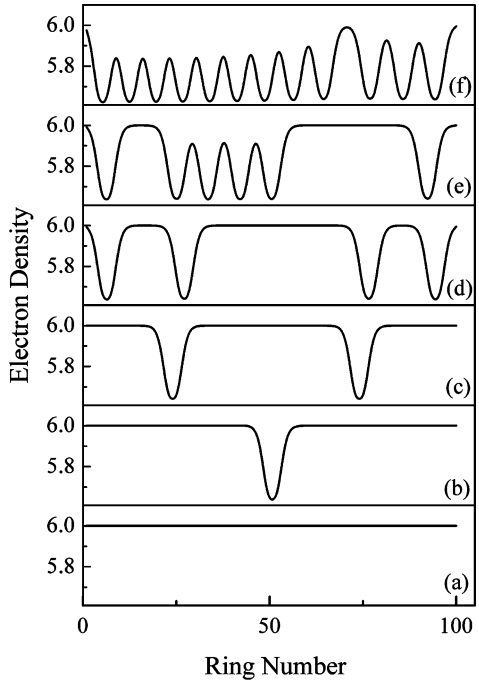

Figure 8. Density of electrons in the different rings of the 100-ring PT chain for bipolaron-doped structures: (a) 0-bipolaron-, (b) 1-bipolaron-, (c) 2-bipolaron-, (d) 4-bipolaron-, (e) 6-bipolaron-, and (f) 12-bipolaron-doped PT chains.

3.3. Geometry Optimization in Doped Polythiophene Oligomers. Doping of PTs creates structurally favored polaronic and bipolaronic defect states responsible for charge storage and excitation. The distortion energies (E_{dis}) of formation for two polarons and one bipolaron are the same, but the decrease in ionization energy is much more pronounced in the case of bipolarons ($2\Delta\varepsilon^{bip}$) than for two polarons ($2\Delta\varepsilon^{pol}$), making one bipolaron more stable than two polarons in these systems.[21]

We have investigated the evolution of structures of bipolaron-doped 100- and 150-ring PT chains containing up to 12 bipolaronic defects. Since there is a large-scale reorganization of geometry following doping, the doped systems provide challenging examples for testing the power of the new technique of geometry optimization introduced here. Let us first inspect what happens when a bipolaronic defect is incorporated into a 100-ring PT chain. Following the creation of a defect (removal of the electron pair from the HOMO), the chain is allowed to relax and the geometrical parameters are globally optimized by using λ-optimized DRMHC in the way mentioned in section 2. The starting geometry is assumed to be identical with the neutral $(PT)_{n=100}$ geometry. The relaxation causes the 2 units of positive charge to spread over the constituent rings of the chain. The charge distributions in neutral and one-bipolaron-doped PT chains of 100 rings are compared in Figure 8a,b. The maximum positive charge is seen to accumulate at the middle of the chain and get distributed on the two sides with near perfect Gaussian symmetry (Figure 8b). When a second bipolaronic defect is incorporated into the 100-ring PT chain, the charge distribution has a two-peak symmetric structure, as if the two defects tend to get separated and localized in two different regions of the chain (Figure 8c). The symmetry is destroyed as more bipolarons are introduced (Figure 8d−f). The one-bipolaron-doped 100-ring PT chain has four clearly

Table 4. Optimized Bond Lengths in 100-, 150-, and 200-Ring Neutral PT Chains[a]

no. of rings	optimized C−S bond length (Å)	optimized C−C bond length (Å)	optimized C=C bond length (Å)	optimized C−C junction bond (Å)
100	1.72152 (1.72153)	1.4405 (1.4406)	1.3492 (1.3493)	1.4569 (1.457)
150	1.72152 (1.72153)	1.4405 (1.4406)	1.3492 (1.3493)	1.4569 (1.457)
200	1.72152 (1.72153)	1.4405 (1.4406)	1.3492 (1.3493)	1.4569 (1.457)

[a] Refer to Figure 1.

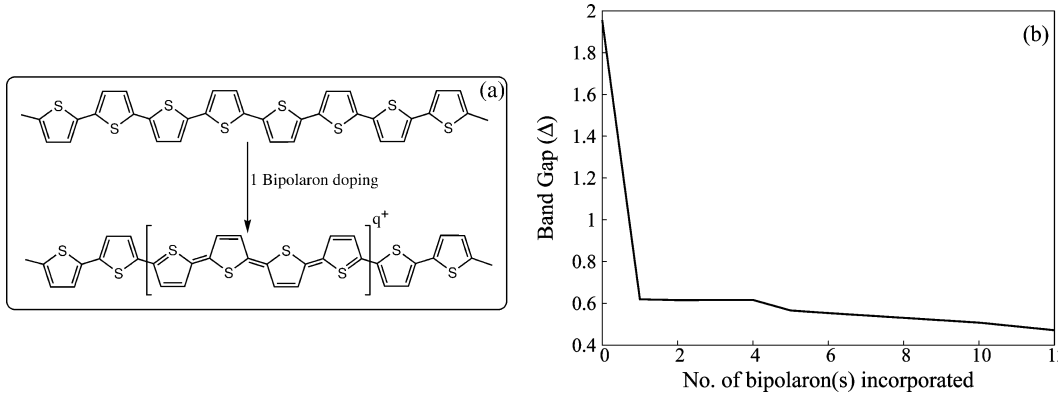

Figure 9. (a) Chemical structure of a one-bipolaron-doped 100-ring PT chain ($q = 1.36$). (b) Reduction of the band gap with the number of bipolarons incorporated into the 100-ring PT chain.

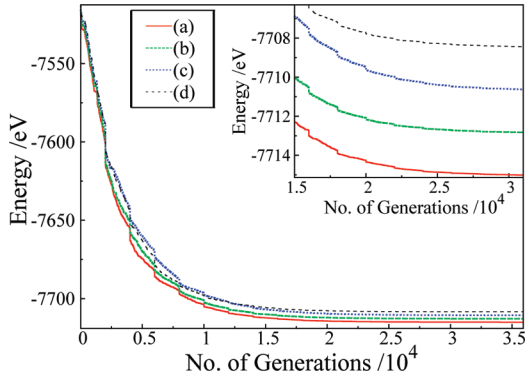

Figure 10. Energy evolution profiles of 150-ring PT chains for a (a) neutral PT chain, (b) two-bipolaron-doped PT chain, (c) four-bipolaron-doped PT chain, and (d) six-bipolaron-doped PT chain. Inset: profile in the region between 15000 and 30000 generations.

quininoid rings in the center containing about 68% of the total charge carried by a bipolaronic defect (Figure 9a). Beyond the 4 rings there is almost a continuous transition to aromatic structure which persists over 13−14 rings. Geometry optimization by the DRMHC procedure thus predicts the expected pattern of evolution of the structures of doped PTs.

The gradual increase in the doping level causes progressive reduction in the band gap, which tends to get saturated at a low but nonzero value (Figure 9b). Incorporation of a single bipolaronic defect drastically brings down the band gap ($\Delta\varepsilon$), and the Fermi level (ε_F) also moves into the valency band. The reduction in the band gap is not so spectacular as the doping level increases further. The lowest value predicted is 0.57 eV for the 12-bipolaron-doped PT chain of 100 rings. It would be of interest to find the optimized structures of bipolaron-doped PTs of even larger chain lengths to test whether our "λ-optimized DRMHC" performs well in this situation. That the geometry optimization in doped PTs proceeds smoothly is shown in representative cases in parts a−d of Figure 10 for 150-ring PT chains with zero, two, four, and six bipolarons, respectively. In each case we have taken the geometry of the neutral PT chain of 150 rings as one starting point which is far from the optimized geometry searched out by our algorithm.

4. Conclusions

λ-optimized directed random mutation hill climbing can be a viable strategy for locating minimum energy structures of undoped as well as doped polythiophenes and their analogues. The algorithm is generizable and can be used to handle the global geometry optimization problem in large molecules with complex potential energy surfaces.

Acknowledgment. K.S. thanks the CSIR, Government of India, New Delhi, for the award of a Junior Research Fellowship. We thank Dr. Pinaki Chowdhury (Calcutta University) for his help.

References

(1) Dykstra, C. E. In *Theory and Applications of Computational Chemistry: The First Forty Years*; Dykstra, C. E., Frenking, G., Kim, K. S., Scuseria, G. E., Eds.; Elsevier: New York, 2005; pp 1011−1045.

(2) Schlegel, H. B. In *Ab Initio Methods in Quantum Chemistry*; Lawley, K. P., Ed.; Advances in Chemical Physics, Vol. LXV11; John Wiley & Sons Ltd.: Chichester, U.K., 1987; pp 1−566.

(3) Cramer, C. J. *Essentials of Computational Chemistry Theories and Models*, 2nd ed.; John Wiley & Sons Ltd.: Chichester, U.K., 2004; pp 487−516.

(4) Kobayashi, M.; Chen, J.; Chung, T. C.; Heeger, A. J.; Wudl, F. Synthesis and properties of chemically coupled poly(thiophene). *Synth. Met.* **1984**, *9*, 77–86.

(5) Logdlund, M.; Lazzaroni, R.; Stafström, S.; Salaneck, W. R.; Bredas, J. L. Direct observation of charge-induced π-electronic structural changes in a conjugated polymer. *Phys. Rev. Lett.* **1989**, *63*, 1841–1844.

(6) Stafström, S.; Bredas, J. L. Evolution of the electronic structure of polyacetylene and polythiophene as a function of doping level and lattice conformation. *Phys. Rev. B* **1988**, *38*, 4180–4191.

(7) Giri, D.; Kundu, K. Theoretical study of the evolution of electronic band structure of polythiophene due to bipolaron doping. *Phys. Rev. B* **1996**, *53*, 4340–4350.

(8) Mazziotti, D. A. Anti-Hermitian contracted Schrödinger equation: Direct determination of the two-electron reduced density matrices of many-electron molecules. *Phys. Rev. Lett.* **2006**, *97*, 143002.

(9) Mazziotti, D. A. Anti-Hermitian part of the contracted Schrödinger equation for the direct calculation of two-electron reduced density matrices. *Phys. Rev. A* **2007**, *75*, 022505.

(10) Gidofalvi, G.; Mazziotti, D. A. Direct calculation of excited-state electronic energies and two-electron reduced density matrices from the anti-Hermitian contracted Schrödinger equation. *Phys. Rev. A* **2009**, *80*, 022507.

(11) Lavadra, F. C.; dos Santos, M. C.; Galvao, D. S.; Lak, B. Insulator-to-metal transition in polythiophene. *Phys. Rev. B* **1994**, *49*, 979–983.

(12) Su, W. P.; Schrieffer, J. R.; Heeger, A. J. Solitons in polyacetylene. *Phys. Rev. Lett.* **1979**, *42*, 1698–1701.

(13) Su, W. P.; Schrieffer, J. R.; Heeger, A. J. Soliton excitations in polyacetylene. *Phys. Rev. B* **1980**, *22*, 2099–2111.

(14) Mitchel, M.; Forrest, S.; Holland, J. H. In *When Will a Genetic Algorithm Outperform Hill Climbing?*; Cowen, J. D., Tesauro, G., Alspector, J., Eds.; Advances in Neural Information Processing Systems, Vol. 6; Morgan Kaufmann: San Mateo, CA, 1994.

(15) Mitchell, M. *An Introduction to Genetic Algorithms*, 1st ed.; MIT Press: Cambridge, MA, 1996; pp 128−132.

(16) Chaudhury, P.; Bhattacharyya, S. P. Numerical solutions of the Schrödinger equation directly or perturbatively by a genetic algorithm: Test cases. *Chem. Phys. Lett.* **1998**, *296*, 51–60.

(17) Sharma, R.; Bhattacharyya, S. P. Direct search for wave operator by a genetic algorithm (GA): Route to few eigenvalues of a Hamiltonian. *Proceedings of the IEEE Congress on Evolutionary Computation, Singapore*; IEEE Press: Piscataway, NJ, 2007; pp 3812−3817.

(18) Nandy, S.; Chaudhury, P.; Sharma, R.; Bhattacharyya, S. P. A density-matrix-based simulated annealing (SA) technique for locating minimum energy structures on the neutral polythiophene potential energy surface. *J. Theor. Comput. Chem* **2008**, *7*, 977–987.

(19) Schaffer, J. D.; Caruana, R. A.; Eshelman, L. J.; Das, R. A study of control parameters affecting online performance of genetic algorithms for function optimization. *Proc. 3rd Int. Conf. Genet. Algorithms* **1989**, 51–60.

(20) Hesser, J.; Manner R. Towards an optimal mutation probability in genetic algorithms. In *Parallel Problem Solving from Nature*; Schwefel, H.-P., Manner, R., Eds.; Lecture Notes in Computer Science, Vol. 496; Springer: Berlin, 1991; pp 23−32.

(21) Bredas, J. L.; Street, G. B. Polarons, Bipolarons, and Solitons in Conducting Polymers. *Acc. Chem. Res.* **1985**, *18*, 309–315.

CT900540D